

INTRODUCTION

In neurons, tight regulation of gene expression is required for proper development and neuronal activity. This occurs at multiple levels – transcriptional regulation, RNA splicing, mRNA transport and localization, and mRNA stabilization play roles in the regulation of key proteins found in neurons. All of these processes occur through interactions between proteins and distinct regions of their target nucleus. In turn, these proteins are themselves regulated by interactions with other proteins.

A well-studied example of mRNA stabilization as a means of regulation in neurons is the stabilization of growth-associated protein-43 (GAP-43) mRNA. GAP-43 is a membrane-bound phosphoprotein with known functions in the development as well as plasticity of the nerve terminal. The *cis*-acting element within the mRNA of GAP-43 was determined through mutagenic studies to be approximately the first 200 nucleotides of the 3' untranslated region (3' UTR) (Perrone-Bizzozero *et al.*, 1993; Nishizawa, 1994). *Trans*-acting factors known to regulate the stability of GAP-43 mRNA has also been studied. A link between extracellular stimuli and GAP-43 mRNA stability was shown with the increased stabilization after NGF stimulation by interaction with cAMP-regulation phosphoprotein-19 (ARPP-19) to the region of the 3' UTR known to regulate the mRNA half-life in a NGF-dependent manner (Irwin *et al.*, 2002). This interaction also depends on the phosphorylation state of ARPP-19 as mutants lacking the known PKA phosphorylation site reduced both basal and NGF-dependent regulation (ibid).

ARPP-19, and its spliceform ARPP-16, were first discovered as protein kinase A (PKA)-dependent phosphoproteins (Horiuchi JBC paper instead Girault *et al.*, 1988). While the only difference between ARPP-19 and ARPP-16 is an additional 16 amino acids at the N-terminus, differences in spatial as well as temporal expression implicate potential differences in function (Girault *et al.*, 1990). Although little is known about the function of these proteins, high conservation from yeast to humans of ARPP-16/19 highlights their importance. Other isoforms included in this family are ARPP-19e and the predicted variant ARPP-19b, which are products of distinct genes. A common feature of this family of proteins is a PKA phosphorylation site located close to the carboxyl terminus (Girault *et al.*, 1988). A central domain is also conserved throughout all species and notably contains a serine that has been shown to be phosphorylated by Rho kinase *in vitro* (Horiuchi & Nairn, unpublished results).

These experiments aim to determine the function and regulation of ARPP-16/19 in neuronal function. To accomplish this, we have utilized a number of different techniques to determine protein interactions as well as indirectly quantify changes at the mRNA level in the absence of these proteins. Also, because its function as an mRNA stabilizing protein in PC12 cells is stimulus dependent, regulation of the phosphorylation sites would provide a connection between extracellular stimulation and mRNA stabilization.

METHODS

Microarray analysis: Conditional knockout ARPP-16/19 animals were generated by mating floxed ARPP-16/19 animals with a *Cre* driver line. RNA from the striata of adult wildtype and conditional knockout males (n=4 each group) was isolated (RNeasy kit, Qiagen). 5µg of total RNA was used for microarray analysis using Affymetrix GeneChip Mouse Genome Array 430 2.0 chips (Yale Microarray Center for the Study of the Nervous System). Analysis of comparisons were done using dChip 2006.

Western blotting analysis: Total and phospho-specific antibodies against ARPP-16/19/e were used at 1:1000 and 1:500, respectively (antibodies gifts from A. Horiuchi, Rockefeller Univ.). Western blotting was performed using standard procedures. Blots were analyzed and quantified using an Odyssey Infrared Imaging System (LiCor, NE, USA).

Subcellular fractionation: Subcellular fractions were isolated as described previously with procedural modifications (Carlini *et al.*, 1980). Briefly, tissue was homogenized using a Dounce tissue grinder in 0.32M sucrose, 20mM HEPES, pH 7.4 with protease and phosphatase inhibitors. Nuclear and unhomogenized cell contaminants were removed by low-speed centrifugation, followed by a high-speed centrifugation to obtain the pellet containing synaptosomes. This was applied to a Percoll gradient (3%, 10%, 23%) and ultracentrifuged. The interface between 10% and 23% was collected and subjected to hypotonic lysis (20mM HEPES, pH 7.4, 1.0mM DTT). Subsequently, the synaptic plasma membrane fraction was collected by ultracentrifugation. Following a detergent treatment (0.32M sucrose, 20mM HEPES, pH 7.4, 0.5% Triton), the PSD fraction was collected by ultracentrifugation and stored at -80°C.

Identification of protein complexes using DIGE: ARPP-16 wildtype, S46D, and S88D proteins were overexpressed in BL21 cells, purified, and immobilized onto Profinity IMAC Ni charged Resin (Bio-Rad, Hercules, CA). The S2 fraction from 11 adult rat striata and hippocampus were precleared with Ni charged Resin, followed by batch-binding to the immobilized ARPP-16 proteins in RNase free conditions for 4 hours in 4°C with shaking. Beads were washed, then eluted with high imidazole. 50 µg of striatal eluent was labeled with Cy3, 50 µg hippocampal eluent with Cy5, and 50 µg pre-clear beads with Cy2 (control). DIGE was performed using Ettan DIGE (Amersham Biosciences). Labeled samples were pooled and isoelectric focusing was performed using a pI range of 3-10. SDS-PAGE on a 12% gel was performed for the second dimension. Dye ratios were determined using DeCyder (Amersham Biosciences). Spots found in the striatal eluent sample, but not the hippocampal or the control were excised and subjected to gel tryptic digestion. Spots were identified using an Applied Biosystems 4800 MALDI-ToF/ToF mass spectrometer. The data was analyzed using the Applied Biosystems GPS Explorer software with Mascot analysis against both the NCBI and IPI mouse databases, and a combined peptide mass fingerprint / MS/MS search was done.

RESULTS

Figure 1: Microarray analysis of ARPP-16/19 conditional KOs show differences at the mRNA level in the striatum

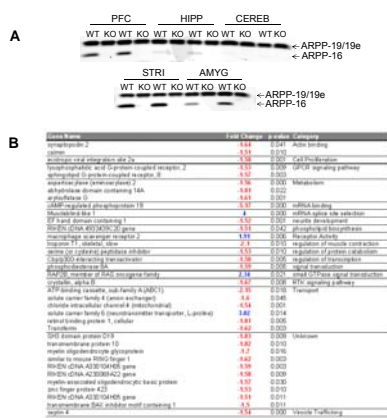


Figure 1: Microarray analysis of conditional ARPP-16/19 knockouts (KOs) vs. wildtypes (WTs). A. Western blot analysis of the conditional ARPP-16/19 KOs in different brain regions showing forebrain-specific knockout. B. Summary of microarray study shows a significant reduction in 4 genes. C. Western blot analysis of Muscblind-like protein -1, -2, and -3 shows a reduction in MLP1 and MLP2 whereas there is a 4-fold increase of mRNA in the ARPP-16/19 KOs.

Figure 3: Inhibition of PP2A/PP1 and PP2B leads to a dephosphorylation of Ser46/61

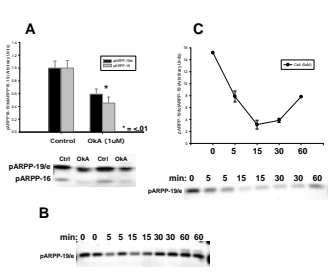


Figure 3: Okadaic acid and cyclosporin A treatment leads to dephosphorylation of Ser46/61 in ARPP-16/19. A. Striatal slices treated with 1µM okadaic acid showed a significant reduction in phosphorylation of Ser46/61 when compared to baseline. B. This reduction is also seen in primary striatal cultures treated with 1µM okadaic acid. C. Striatal slices treated with 5µM cyclosporin A showed a reduction in phosphorylation of Ser46/61 when compared to baseline.

Figure 2: DIGE analysis of interacting partners with ARPP-16 and phosphomimetics show possible differential interactions in different phospho states

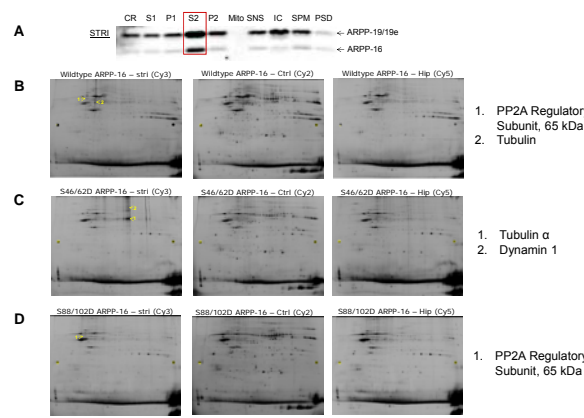


Figure 2: Determination of proteins complexed with ARPP-16 specifically in the striatum. A. Subcellular fractionation in rat striatum reveals ARPP-16/19e localization in the cytosolic fraction (S2). B. Wildtype ARPP-16 pull-down DIGE images. 175 spots were picked, 26 were analyzed, 10 were IDed, 2 were unique to the striatal eluent. C. S46D-ARPP-16 pull-down DIGE images. 226 spots were picked, 37 were analyzed, 7 were IDed, and 2 were unique to the striatal eluent. D. S88D-ARPP-16 pull-down DIGE images. 216 spots were picked, 29 were analyzed, 7 were IDed, and 1 was unique to the striatal eluent.

Figure 4: Activation of PKA by forskolin leads to a dephosphorylation of Ser46/61

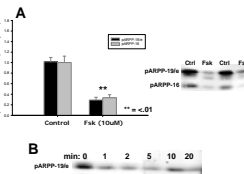


Figure 4: Forskolin treatment leads to dephosphorylation of Ser46/61 in ARPP-16/19. A. Striatal slices treated with 10µM forskolin showed a significant reduction in phosphorylation of Ser46/61 when compared to baseline. B. This reduction is also seen in primary striatal cultures treated with 10µM forskolin.

Figure 6: Inhibition of ser/thr kinases leads to phosphorylation of Ser46/61

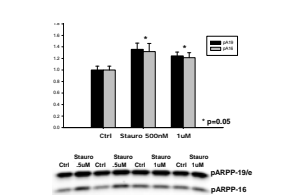


Figure 6: Staurosporin treatment leads to increased phosphorylation of Ser46/61 in ARPP-16/19. Striatal slices treated with 500nM and 1µM staurosporin showed a significant increase in phosphorylation of Ser46/61 when compared to baseline.

Figure 5: Both NMDAR and DIR activation leads to dephosphorylation of Ser46/61

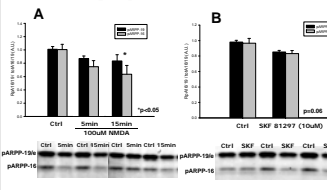


Figure 5: NMDA and SKF 81297 treatment leads to dephosphorylation of Ser46/61 in ARPP-16/19. A. Striatal slices treated with 100µM NMDA showed a significant reduction in phosphorylation of Ser46/61 when compared to baseline. B. Striatal slices treated with 10µM SKF 81297 also showed a reduction in phosphorylation of Ser46/61.

Figure 7: Contrary to previous *in vitro* phosphorylation studies, ARPP-16/19 is not a Rho Kinase substrate at Ser46/61

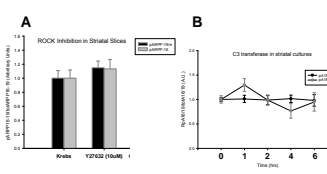


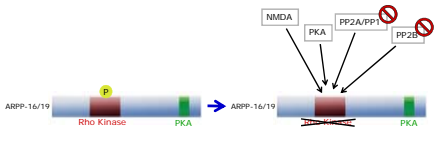
Figure 7: Y27632 and C3 transfectase treatment show no difference in phosphorylation at Ser46/61. A. Striatal slices treated with 1µM Y27632 showed no difference in phosphorylation of Ser46/61 when compared to baseline. B. Primary striatal cultures treated with 2.5µg/ml C3 transfectase also showed no difference.

CONCLUSIONS

Microarray analysis of ARPP-16/19 conditional knockout animals shows a reduction in mRNA levels of a number of genes, which is consistent with an mRNA stabilizing protein.

DIGE studies using wildtype and phosphomimetic mutants of ARPP-16 show differences in interactions when comparing spot patterns between the three proteins. This may indicate differential interactions depending on phosphorylation state.

Phosphorylation of ARPP-16/19 at Ser46/61 is highly phosphorylated at baseline and sensitive to dephosphorylation by a number of different agents. This can either be due to a phosphatase or a kinase inhibitor that is activated by PKA and NMDAR signaling and inhibited by PP2A/PP1 and PP2B.



METHODS (continued)

Striatal slice preparation: Striatal slices were prepared as described with slight procedural modifications (Nishi *et al.*, 1997). The brains were rapidly removed and placed in ice-cold, oxygenated Krebs-HCO3 buffer (124 mM NaCl, 4 mM KCl, 26 mM NaHCO3, 1.5 mM CaCl2, 1.25 mM KH2PO4, 1.5 mM MgSO4, 10 mM d-glucose, pH 7.4). Coronal slices (350 µm) were prepared using a vibrating blade microtome (VT1000S, Leica Microsystems). Striata were dissected from the slices and then placed in a polypropylene incubation tube with 2 ml of fresh Krebs-HCO3 buffer and allowed to recover for 30 min with constant oxygenation with 95% O2/5% CO2 at 30°C followed by another 30 minutes of recovery with adenosine deaminase added to fresh Krebs-HCO3 buffer.

Primary striatal cultures: Rat postnatal striatal cultures were prepared as described with slight procedural modifications (Malgaroli & Tsien, 1992). Briefly, the striata of P1 rat pups were excised in dissection medium (HBSS, 10mM HEPES, 33.3mM Glucose, 2 mM CaCl2, 0.3% BSA, 12mM MgCl2, 2% Pen-Strep, pH 7.4), minced and digested in digestion solution (4.2 mM NaHCO3, 25mM HEPES, 137 mM NaCl, 5mM KCl, 7 mM Na2HPO4, pH 7.4, 0.1% papain) for 1 hour at 37°C. Afterwards, the cells were triturated and cultured in Neurobasal-A (B27, Glutamax 1, 1 mM HEPES, 2% Pen-Strep, pH 7.4) with 5% FBS for one day, then Neurobasal-A without serum for 20 DIV.

REFERENCES

Carlini, R.K., Grab, D.J., Cohen, R.S., Siekevitz, P. *J Cell Biol.* 1980 Sep;**86**(3):831-45.
Girault, J.-A., Shalaby, I.A., Rosen, N.L., Greengard, P. *Proc Natl Acad Sci USA.* 1988 Oct;**85**(20):7790-4.
Girault, J.-A., Horiuchi, A., Gustafson, E.L., Rosen, N.L., Greengard, P. *J Neurosci.* 1990 Apr;**10**(4):124-33.
Irwin, N., Chao, S., Goritschenko, L., Horiuchi, A., Greengard, P., Nairn, A.C., Benowitz, L.L. *Proc Natl Acad Sci U S A.* 2002 Sep 17;**99**(19):12427-31.
Nishi, A., Snyder, G.L., Greengard, P. *J Neurosci.* 1997 Nov 1;**17**(21):8147-55.
Nishizawa, K. *Biochem Biophys Res Commun.* 1994 Apr 29;**200**(2):789-96.
Perrone-Bizzozero, N.I., Cansino, V.V., Kohn, D.T. *J Cell Biol.* 1993 Mar;**120**(5):1263-70.

Acknowledgements

The authors would like to acknowledge Fan-Yan Wei, Hideo Matsuzaki, and Dilja Krueger for their help with this work.

SUPPORT

Yale/NIDA Neuroproteomics Research Center 1 P30 DA018343-0 (TW, KS, ACN), NIDA grant DA10044 (ACN), NINDS grant 1U24NS051869 (SM)